



**Environmental
Science**
Water Research & Technology

**Effects of an anaerobic membrane bioreactor upset event on
nitrogen speciation and microbial community in a
downstream phototrophic membrane bioreactor**

Journal:	<i>Environmental Science: Water Research & Technology</i>
Manuscript ID	EW-ART-12-2024-000987.R1
Article Type:	Paper

SCHOLARONE™
Manuscripts

Water Impact Statement

A transient event in anaerobic membrane bioreactor effluent quality influenced the chemistry and microbiology of a downstream phototrophic membrane bioreactor. However, the membrane separation element allowed for recovery of the microbial community once the transient event passed. Understanding failure modes is imperative for future implementation of membrane bioreactors, especially as it relates to remote, resource-limited environments.

Effects of an anaerobic membrane bioreactor upset event on nitrogen speciation and microbial community in a downstream phototrophic membrane bioreactor

Daniella Saetta^{a*}, Jason A. Fischer^b, Ashley Triana^c, Talon Bullard^c, Alexandra Smith^c, Cory J. Sperrn^d, Anirudha Dixit^b, Christina L. Khodadad^d, Daniel H. Yeh^c, and Luke B. Roberson^e.

^aBennett Aerospace, Inc.,
Kennedy Space Center, FL, 32899, USA

^bAetos Systems, Inc.,
Kennedy Space Center, FL, 32899, USA

^cDepartment of Civil and Environmental Engineering Department,
University of South Florida,
4202 E. Fowler Ave. ENG 030, Tampa, FL, 33620, USA

^dNoetic Strategies,
Kennedy Space Center, FL, 32899, USA

^eNational Aeronautics and Space Administration,
Kennedy Space Center, FL, 32899, USA

* Corresponding Author
Tel: 1-954-557-6182
E-mail Address: Daniella.saetta@nasa.gov (D. Saetta)

Submitted to

Environmental Science: Water Research & Technology

24 Jan 2025

1 **ABSTRACT**

2 A wastewater treatment architecture with an anaerobic membrane bioreactor and a phototrophic
3 membrane bioreactor was created to close resource loops for use on the Moon and Mars. During
4 an anomaly, an increase of carbon-to-nitrogen ratio led to a shift in the microbial community
5 within PMBR. It is imperative to understand failure modes of the system and the system's ability
6 to respond to perturbations in treatment because of their proposed application in remote,
7 resource-limited locations. During this transient event, the carbon-to-nitrogen ratio in the
8 AnMBR permeate increased from 0.341 to 11.2. Results showed that the microbial community
9 became more diverse during the event and enriched in species related to the remediation of
10 aromatic compounds. The community shift led to conditions required for greater than 90%
11 carbon removal by the PMBR. The inclusion of the PMBR in the treatment architecture
12 increased resilience and robustness for treating high-strength wastewaters in extreme
13 environments.

14 **1. Introduction**

15 Technology development for decentralized wastewater treatment has been increasing as a means
16 for providing access to sanitation in rural, resource-limited, underserved, marginalized, and
17 aging communities. Decentralized wastewater treatment is challenged to its most extreme realms
18 when designed for extraplanetary, partial gravity habitats, such as those planned for the Moon
19 and Mars. The wastewater treatment technology development community has identified
20 anaerobic digestion (AD) as an alternative to conventional activated sludge wastewater
21 treatment, especially in decentralized contexts.¹ When coupled with membrane filtration, AD can
22 be applied to high-strength wastewaters with a small treatment footprint.² Anaerobic membrane
23 bioreactors (AnMBRs), which is AD coupled with membrane filtration, allow for a decoupling
24 of solids and hydraulic retention times, which increases treatment rates, chemical oxygen

25 demand (COD) removal between 76–99%, and total suspended solids (TSS) removal higher than
26 99%.^{2,3} This allows for further reduction in the treatment footprint, reinforcing their applicability
27 for decentralized communities. Moreover, AnMBRs can also produce biogas, composed mainly
28 of carbon dioxide and methane, which can be recovered to offset energy requirements.⁴
29 However, AnMBRs are limited by their inability to remove nutrients and in some cases, such as
30 in municipal wastewater treatment, downstream technologies are proposed for nutrient removal.⁵
31 In AnMBRs, nitrogen and phosphorus, in the form of ammonium and phosphate, are released
32 into the water phase as solids are hydrolyzed.⁶ This can be used as an asset in nutrient recovery
33 applications, such as fertigation systems, because the nutrients are released in a more usable
34 form. However, high-ammonium waters have higher rates of nitrogen loss and are not preferable
35 for fertigation systems, as ammonium has a large impact on solution pH when plants release H⁺
36 ions after absorbing NH₄⁺ to maintain solution neutrality.^{7,8}

37 Researchers propose the use of algae-based MBRs, also known as phototrophic
38 membrane bioreactors (PMBRs), as a secondary treatment for AnMBR permeates because of
39 their ability to remove excess nitrogen, phosphorus, and COD.^{9,10} If seeded with an algal–
40 bacterial consortium, oxygen produced by the algae can be used by nitrifiers during nitrification
41 and the system can act as a nitrate recovery technology.^{11,12} Studies have shown that the presence
42 of algae increases the rate of nitrification and ammonia uptake by the microalgae due to the
43 oversaturation of dissolved oxygen.¹³ Yet, the algal and bacterial communities need to be
44 balanced to form a symbiotic relationship that does not create conditions that limit the other.

45 The balance between algae and bacteria can be influenced by the following parameters:
46 (1) influent nitrogen form and concentration, (2) temperature, (3) light, (4) carbon concentration
47 in the influent, (5) pH, (6) oxygen concentration, and (7) hydraulic and solid retention times.^{14,15}

48 Of the seven parameters identified by Gonzalez-Camejo et al., five parameters can be
49 manipulated via the control software and hardware operating the system. The operational
50 software and hardware of a PMBR is not able to control the concentration of carbon or the
51 nitrogen speciation and concentration in its influent, as that is dependent on the operation of the
52 system treating and supplying the influent. Nitrogen speciation in the PMBR influent is
53 independent of the control system and it influences the efficiency of nitrogen removal, as
54 systems have been shown to have higher removal efficiencies when treating 100% NH_4^+ versus
55 100% NO_3^- .¹⁶ However, while the concentration of ammonia may increase or decrease, the
56 nitrogen speciation was not expected to change from NH_4^+ to NO_3^- at any point of the study, as
57 the conditions for nitrification were not provided in the AnMBR. Conversely, if carbon is added
58 to PMBRs in excess, fast-growing bacteria can flourish and block light penetration required for
59 the algae to perform photosynthesis.¹⁷ There is a gap in the literature surrounding the response of
60 algal–bacterial PMBRs to perturbations in upstream treatments. It is important to understand
61 failure modes and responses to perturbations with AnMBR and PMBR technology, especially
62 because they have been proposed as solutions for low-resource and remote locations, and
63 because the likelihood of perturbations occurring is plausible in real-world applications. In
64 general, the functional stability of bioreactors can be influenced by three important factors: (1)
65 functional diversity within the microbial community, (2) evenness of the community leading to
66 robustness, and (3) population dynamics governed by resistance, resilience, and redundancy of
67 the community when facing perturbations.¹⁸ Research related to failure modes of
68 photobioreactors for application in outer space has identified bacterial competition as a critical
69 failure mode, among other failure modes related to improper illumination, insufficient CO_2 , and
70 exposure to elevated radiation.¹⁹ Failure mode analysis is a critical element in future planning of

71 space exploration, and this type of research can inform stakeholders on a failure mode related to
72 culture robustness during a stress event.

73 In this research, an architecture with AnMBR followed by a PMBR was designed as
74 bioregenerative life support systems (BLiSS) for planetary habitats on the Moon and Mars.²⁰ The
75 AnMBR would serve as a carbon removal technology and the PMBR would serve as a nutrient
76 polishing technology, with carbon removal being the primary goal and nutrient recovery for
77 fertigation of crops being a secondary goal. AnMBR and PMBR technologies are suitable for
78 application on the Moon and Mars because they do not depend on chemical inputs, have a small
79 footprint, and high treatment efficiencies.²¹ As opposed to terrestrial wastewater treatment
80 systems, nutrients are recovered for reuse in BLiSS architectures, because the nutrient stream is
81 seen as a resource that would otherwise need costly resupply from Earth.²² Once a BLiSS is
82 integrated into the habitation systems, the astronauts need to have a reliable and robust system
83 that will provide its intended services, which may include wastewater treatment, water recovery,
84 and nutrient delivery for fertigation of crops. Additionally, because these systems are designed to
85 treat wastewater in parallel, the latter system should not produce an effluent that diminishes the
86 quality of the primary system, such as increasing the chemical oxygen demand (COD) or total
87 suspended solids (TSS) concentrations in this case. Therefore, the goal of this study was to
88 provide an improved understanding of AnMBR and PMBR operations during off-nominal
89 periods of increased organic carbon loading for an improved understanding of failure modes as
90 they pertain to application in extreme environments. The specific objectives of the research were
91 to (1) describe the transient event that caused off-nominal upstream conditions in the AnMBR
92 permeate, (2) detail the water quality and treatment parameters in the PMBR during operation
93 before and after the transient loading event, (3) identify the microbial communities present in the

94 mother culture, during, and after the transient event, and (4) discuss reliability and robustness of
95 these systems in terms of their application for Lunar and Martian partial gravity habitats.

96 **2. Materials and Methods**

97 **2.1. Anaerobic membrane bioreactor**

98 A 54 L AnMBR was designed to reduce chemical oxygen demand and to liberate nutrients in
99 high-strength organic waste with the main goal of closing the water and nutrient cycles on
100 planetary bases (see Figure S1 for reactor schematic).^{21,27} The system described in this research
101 was designed to continuously treat the waste produced by 4 crewmembers.²⁷ The AnMBR
102 consisted of 3 sequential tanks prior to membrane filtration to allow for phased digestion. The
103 buffer tank acted as a flow equalization tank prior to the anaerobic digestion tanks. Reactor tank
104 1 (R1) and reactor tank 2 (R2) were seeded with anaerobic digestion sludge collected at a local
105 wastewater treatment plant. The contents of R2 were circulated through an PVDF hollow fiber
106 ultrafiltration (UF) membrane (0.199 m² membrane surface area), where solids were retained and
107 the nutrient-rich liquid permeate was recovered. The headspace in the BT, R1, and R2 tanks were
108 interconnected and the combined biogas created by the culture was routed to a gas meter that
109 measured the daily biogas production. A lag in biogas production was expected due to the period
110 needed for the sludge to acclimate to a new environment with a lower temperature (room
111 temperature vs. 35°C) and a new wastewater source. During this study, the AnMBR treated 2.5
112 L/d of a fecal wastewater ersatz called complex organic particulate artificial sewage (COPAS) at
113 a 5% solids concentration.²⁸ COPAS is an easily reproducible ersatz that uses milled cat food
114 pellets as the source of proteins, carbohydrates, and particulate matter at concentrations similar
115 to those found in fecal matter. COPAS was made by mixing 50 g/L of the milled cat food with
116 tap water to a desired volume. The AnMBR had been used for three runs prior to the study

117 period described in this paper. A run was defined as the period of operation after each R1 and R2
118 tank reseed event. The length of time between reseeding events varied but three runs took place
119 in the 487 days prior to this study period.

120 **2.2. Phototrophic membrane bioreactor**

121 A 6 L phototrophic membrane bioreactor (PMBR) was used to treat the AnMBR permeate. The
122 PMBR consisted of a flat-plate photobioreactor with a PVDF hollow fiber UF membrane (0.083
123 m² membrane surface area) for permeate production. The design elements have been described in
124 Saetta et al, 2022.¹¹ The PMBR was designed to treat 2.5 L/d of AnMBR permeate. The system
125 architecture, including the AnMBR and PMBR, is shown in Figure S1. The AnMBR permeate
126 was stored in a reservoir tank (RT) between the AnMBR and the PMBR. A buffer volume of
127 approximately 15 L was accumulated in the RT to allow the PMBR to continue operation during
128 scheduled or unscheduled maintenance events of the upstream AnMBR. Two level sensors were
129 installed on the RT to allow for communication between the AnMBR and the PMBR. A low-
130 level sensor indicated (to the PMBR) that the liquid level in the RT was below acceptable limits
131 and would, therefore, stop the PMBR feed pump. A high-level sensor indicated (to the AnMBR)
132 that the RT was full and would, therefore, stop the AnMBR from pumping permeate into the RT.
133 This tank had an HRT of about 6 days.

134 An algal-bacterial culture was used to seed the PMBR. *Chlorella sorokiniana* (UTEX B
135 2805) was used as the starting microalgae species for the mother culture. The algae culture was
136 initially grown in an ammonia-based growth medium. The recipe of the ammonia-based medium
137 was created based on values described in the literature.^{23–26} It had an ammonium (NH₄⁺)
138 concentration of 169.6 mg/L and a C/N ratio of 0.16. The medium recipe is provided in Table
139 S1. The mother culture was grown in a 5 L bottle with mixing at 125 RPM, constant temperature

140 (30°C), and constant light (400 $\mu\text{mol}/\text{m}^2/\text{s}$) (Heliospectra Elixia, LX601C grow light). Room air
141 was continuously pumped into the bottle at a flow rate of 1 L/min. The bottle was sealed and the
142 air delivery was filtered through a 0.22 μm PTFE filter, but other aseptic methods were not
143 followed when handling the culture. This allowed for a consortium of algae and bacteria to grow
144 in the mother culture. Weekly feeding of the mother culture consisted of removing $\frac{1}{4}$ of the
145 culture volume and replacing it with an equal volume of the ammonia-based medium. The
146 mother culture was fed in this manner for 1.5 years prior to the beginning of this study period.
147 The PMBR was seeded with a mixture of the mother culture and tap water to a measured optical
148 density of 1 at 680 nm at the beginning of the experiment.

149 **2.3. AnMBR and PMBR Operations**

150 The AnMBR and PMBR were operated continuously during this study. That meant that the
151 AnMBR system was treating 2.5 L/d of COPAS and the PMBR was treating 2.5 L/d of AnMBR
152 permeate during periods of nominal operation. Off-nominal events, such as failures with pump
153 hardware, led to short periods of treatment below 2.5 L/d. However, the system was operating at
154 2.5 L/d for more than 90% of the study period. The system controller activated the respective
155 influent pumps based on level sensors at the top of the reactor volumes, i.e., the top of BT, R1,
156 R2, and the PMBR reactor tanks. Therefore, the membrane permeate pump flow rate on the
157 PMBR was used to control the flow rate of the entire system because a low level in the PMBR
158 reactor would draw contents from RT and the low level on RT would lead to permeate
159 production in the AnMBR. During nominal operations, 2.5 L/d (membrane flux of 1.21 L/h/m²)
160 of PMBR permeate was produced. Daily average transmembrane pressure (TMP) for each
161 membrane was calculated using data collected every 30 min.

162 The nominal HRT for the system and subsystems was calculated via the following
163 equation: $HRT = V/Q$, where V = volume of the reactor; Q = flow rate. During nominal
164 operations, the combined HRT for the AnMBR and PMBR was approximately 37.2 days. Each
165 tank in the AnMBR had an HRT of 7.2 days, equaling an HRT of 21.6 days for treatment in the
166 AnMBR. The PMBR had an HRT of 2.4 days. The additional days in the HRT for the entire
167 system were attributed to the time spent in the AnMBR permeate tank and the RT. The HRT
168 contributed to the difference in concentrations from tank to tank and from reactor to reactor. As
169 the fluids moved from tank to tank, they were first diluted by the contents in the tank until they
170 had replaced the entire contents of the tank over time. During periods of off-nominal flow rates,
171 such as the transient event described in this paper, the HRT was decreased and more permeate
172 was produced than intended, leading to a shortened treatment time in the R1 and R2 tanks and
173 insufficient time for complete anaerobic digestion to take place. In this study, incomplete
174 anaerobic digestion was defined as periods of less than 90% COD removal and less than 5 L/d of
175 biogas production. Transient events would have impacts on the reactor conditions, such as
176 elevated dissolved concentrations of constituents and elevated solids concentrations.

177 A full-spectrum LED grow light (Mars Hydro, TSW 2000) was used to illuminate the
178 PMBR surface area with a light intensity of $450 \mu\text{mol}/\text{m}^2/\text{s}$. During the first half of the study, the
179 light was delivered in 12 light/dark cycles, with a cycle being a 2-hour light followed by a 2-hour
180 dark period. On day 72, the light cycles were changed to a 3-hour light and 1-hour dark
181 photoperiod for the duration of the study as a strategy to increase the algal population. The
182 PMBR had an illuminated surface area of approximately 1311 cm^2 (203.25 in^2). The temperature
183 in the reactor was controlled at 30°C . Carbon dioxide was introduced in the PMBR at a flow rate
184 of 1 L/min into the bottom half of the reactor and bubbled through the left side of the reactor

185 before it was released through the CO₂-out port to be recycled through a CO₂ recycle subsystem.
186 In a controlled mixing chamber, the recycled CO₂ from the reactor was mixed with CO₂ from a
187 k-bottle to maintain the CO₂ concentration at 3000 ppm, which is the average concentration of
188 CO₂ in the cabin air of the International Space Station (ISS).²⁹ This concentration was chosen
189 because the CO₂ for the PMBR would come from the cabin air or a cabin air CO₂ removal
190 technology in the proposed architecture for the Moon and Mars.

191 **2.3.1. AnMBR and PMBR sampling**

192 Daily samples of oxidation-reduction potential (ORP) of R1 and R2 were taken to assess
193 anaerobic performance. Weekly samples were taken from eight locations: (1) the AnMBR
194 Influent tank, (2) the BT, (3) R1, (4) R2, (5) the AnMBR membrane permeate, (6) the reservoir
195 tank (RT), (7) the PMBR reactor contents (PMBR), and (8) the PMBR membrane permeate.
196 About 100 mL were taken at each location. The samples were divided into total and soluble
197 fractions for future analysis. The soluble samples were prepared by centrifuging 50 mL for 15
198 min at 3400 rpm. The remaining 50 mL were designated as the total fraction (used to measure
199 TSS and COD). The soluble fractions were used to measure soluble COD, dissolved organic
200 carbon (DOC), total nitrogen (TN), total phosphate (TP), and ammonia-nitrogen. Samples were
201 stored at 4°C until analysis took place. All sample analyses were conducted within a week of
202 sample collection and methods are detailed in Section 2.4.

203 Whole genome sequencing samples were taken for three sample types: (1) the mother
204 culture used to inoculate the reactor, (2) the reactor contents and attached biofilms during the
205 peak in the transient event (day 101), and (3) the reactor contents post transient event (day 161).
206 The biofilm samples were taken from the area around the port where the AnMBR permeate was
207 introduced into the PMBR (called the “Biofilm Feed Corner” sample), the area around the float

208 switch used for level sensing (called the “Biofilm Float Switch” sample), and the area around the
209 port where the membrane recirculation was reintroduced into the reactor (called the “Biofilm
210 Recirc Corner” sample). Only reactor contents were sampled for the time point after the reactor
211 recovered from the transient event because the thick biofilms were no longer present. The
212 methods used for DNA sequencing and analysis can be found in Saetta et al., 2023.³⁰ Briefly,
213 whole genome sequencing was performed on DNA samples extracted with Qiagen’s DNeasy
214 PowerLyzer PowerSoil Kit. Illumina Miseq was used to sequence samples, Kraken2 was used to
215 analyze the data, and PlusPFP (a pre-built RefSeq database) was used to map archaea, bacteria,
216 viral, human, UniVec_Core, protozoa, fungi, and plant taxonomic information. The alpha
217 diversities (Shannon diversity index) and beta diversities (Bray-Curtis dissimilarity) on the entire
218 dataset were calculated with the Kraken2 tools.

219 **2.4. Analytical methods**

220 The ORP of R1 and R2 was measured using a handheld ORP meter (MW500, Milwaukee
221 Instruments). The optical density (OD) of the PMBR reactor culture was measured with a 1 cm
222 pathlength cuvette on a visible spectrophotometer (Thermo Spectronic Genesys 20) at a
223 wavelength of 680 nm. TSS of the AnMBR reactor contents was measured with the Standard
224 Method 2540 D. Chemical analysis was conducted using Hach Test ‘N Tube methods for TN,
225 TP, ammonia-nitrogen (NH₃-N), nitrate-nitrogen (NO₃-N), and nitrite-nitrogen (NO₂-N) using
226 the spectrophotometer mentioned above. DOC was measured using an OI Analytical Aurora
227 1030 TOC analyzer. COD was measured using Hach COD Digestion Vials in the high range. In
228 the PMBR reactor, dissolved oxygen concentration (optical DO sensor), pH (Pinpoint pH,
229 American Marine Inc.), and CO₂ concentrations (K30 10,000 ppm CO₂ Sensor, CO2Meter.com)
230 were measured continuously and recorded every 5 min by an Opto 22 controller.

231 **2.6. Carbon-to-nitrogen ratio and nitrogen mass balance**

232 The carbon-to-nitrogen ratio in the AnMBR permeate and the RT was calculated using the DOC
233 and TN concentrations in the weekly samples. The concentrations were converted to molar
234 concentrations prior to calculating the ratio. A weekly nitrogen balance was calculated using the
235 weekly concentrations of TN, NH₃-N, NO₃-N, and NO₂-N. The NH₃-N, NO₃-N, and NO₂-N
236 concentrations were converted to molar nitrogen concentrations before being normalized by the
237 molar TN concentration for that weekly sample. The mass balance was calculated for the
238 dissolved and colloidal fraction, due to the presence of the UF membrane. The dissolved fraction
239 was defined as the concentration of the nitrogen species in the membrane permeate samples
240 (dissolved nitrogen that passes through the membrane). The colloidal fraction was defined as the
241 difference between the nitrogen species concentrations in the PMBR reactor samples and the
242 permeate samples (nitrogen colloids rejected by the membrane). For example, the colloidal NO₃-
243 N fraction was calculated as the difference between the NO₃-N in the PMBR permeate sample
244 and the NO₃-N in the PMBR reactor sample. The dissolved and colloidal fractions were
245 calculated for each weekly concentration of the nitrogen species (NH₃-N, NO₃-N, and NO₂-N)
246 and it was normalized by the TN in the influent sample (RT).

247 **3. Results and Discussion**

248 **3.1. Description of the AnMBR transient event**

249 The AnMBR, used to treat organic waste, was in nominal operation prior to day 30. Nominal
250 operation was defined as production of a low-carbon, high-nutrient permeate for downstream use
251 while treating 2.5 L/d of the organic simulant wastewater (see Table S2 for average influent
252 concentrations). Specifically, permeate samples were monitored to confirm nominal operation
253 with COD removal above 95%, TSS removal above 90%. Additionally, daily samples for ORP

254 were taken to ensure that anaerobic conditions were maintained in the reactor tanks and daily
255 biogas production was tracked to ensure that more than 5 L/d were being produced. On the days
256 leading up to day 38, the operators noticed that the permeate production rate was decreasing at
257 the set permeate pump flow rate and TMP was increasing in the AnMBR membrane (see
258 timeline of events in Figure S2; see TMP data in Figure S3). Due to fouling over time, the flow
259 rate of the permeate pump had been slowly increased over its lifetime to maintain the production
260 of 2.5 L/d of permeate. On day 38, a decision was made to install a new membrane module on
261 the AnMBR. The original membrane module was installed 487 days prior to this reactor run and
262 it had reached the end of its life. Upon installing the new membrane module, an operator error
263 was made when the permeate pump flow rate was not reduced to match the state of the new
264 membrane. With the new membrane module and the elevated flow rate, more than 2.5 L/d of
265 permeate was produced, and contents from the feed tank were pushed through the system at a
266 faster rate. The shortened HRT led to an increase in feed rate to the AnMBR, an increase in TSS
267 in the BT and R1, and increased carbon in the permeate due to insufficient treatment time in R1
268 and R2. The elevated flow rate was kept in operation for 4 days, which delivered the 10 L
269 available in the feed tank into the system and produced permeates from the additional volume
270 available in BT, R1, and R2 before the tanks reached the low-level sensors and the operating
271 software stopped the production of permeate. It is impossible to calculate the actual HRT during
272 this period because the actual flowrate was not known but it could have been as low as 5.4 d if
273 the entire feed tank was introduced in one day (nominal HRT was 21.6 d). After the four days,
274 the flow rate was restored to 2.5 L/d and sampling of the tanks continued to assess the health of
275 the reactor as scheduled.

276 The transient event had direct (DOC, COD, ORP, daily biogas production, and TP) and
277 indirect (TSS, TN, and TMP) effects on the AnMBR microbiology and chemistry. In terms of
278 anaerobic conditions, between day 0 and day 38, the ORP of R1 and R2 were within ranges
279 expected for anaerobic conditions, with levels below -100 mV in R1 and below -300 mV in R2
280 (see Figure S4). However, the ORP in R2 increased to -250 mV on day 44 and then slowly
281 decreased back to nominal levels below -300 mV from day 64 until the end of the study.
282 Additionally, the reactor started producing more than 5 L/d of biogas on day 24, with it
283 averaging about 16 L/d for the following 6 days (see Figure S5). Interestingly, the period of
284 production difficulties that led to changing the membrane module can be seen in the biogas data,
285 as the daily biogas production started decreasing on day 30 and reduced to 0 L/d on day 33 and
286 the transient event started on day 38. As seen in Figure 1a, prior to day 38, the AnMBR permeate
287 had an average DOC concentration of 98.3 mg/L, showing that the system was able to reduce the
288 DOC by greater than 95%. A small increase was seen in the total COD (Figure 1b) of the
289 permeate on day 20. However, the COD concentration in the permeate recovered to 123 mg/L
290 total COD in the weekly samples immediately following the increase. On day 42, an increase is
291 seen in the AnMBR permeate DOC and COD, indicating that the transient event had altered the
292 chemistry of the AnMBR and more carbon was being released in the permeate than in previous
293 weeks. At the peak of the transient event (day 56), the permeate concentrations increased to
294 about 3200 mg/L DOC and 9200 mg/L COD. The AnMBR produced 0 L/d of biogas until day
295 50, and then production started to slowly (between 0–3 L/d). The daily biogas production
296 increased steadily from that moment on, peaking with 30.9 L on day 136, and correlated to the
297 decreasing COD concentrations in the reactor tanks as the effects of transient event passed
298 through the system. The final direct effect of the transient event can be seen in the TP

299 concentration in the permeate samples (see Figure S6). In AnMBRs, phosphate is released into
300 solution as the wastewater solids are hydrolyzed.⁵ However, increased pH, alkalinity, and
301 ammonia concentrations within AnMBR systems can lead to precipitation of phosphate-
302 containing minerals, such as struvite ($\text{MgNH}_4\text{PO}_4 \cdot 6\text{H}_2\text{O}$), and to an accumulation of phosphate
303 in the sludge.^{31,32} Prior to the transient event, the TP in the permeate was about 4x lower than the
304 influent concentration. However, after the transient event, the concentrations of the influent and
305 permeate were within 100 mg/L of each other. This was indicative that decreased HRT did not
306 create the conditions necessary for phosphate precipitation that was seen prior to the transient
307 event.

308 Analysis of the TSS concentrations was also used to determine if the reactor tanks had
309 been overloaded with solids as a result of a decrease in HRT. The data show that the permeate
310 TSS concentrations stayed low, as expected for a functioning membrane (Figure 1c). However,
311 the TSS concentration in the BT increased from 35,000 mg/L on day 34 to 110,000 mg/L on day
312 42. That increase in the TSS in BT slowly impacted the TSS in R1, which made its way through
313 the system and impacted the TSS concentrations in R2. The TSS in R1 reached levels above
314 22,000 mg/L on day 84 and the TSS in R2 reached levels above 14,000 mg/L on day 91. The
315 increasing TSS also had an impact on the AnMBR membrane module, with the TMP increasing
316 from about 0.25 bar to about 0.75 bar and fluctuating in that range for the remaining days of the
317 study (Figure S3).

318 The TN concentration followed a similar trend to TSS due to the inherent mechanisms of
319 anaerobic membrane bioreactors. In AnMBR technology, the nutrients trapped in the solid phase
320 are slowly solubilized by the microorganisms in the reactor. This solubilization releases the
321 nutrients into the water phase, which can be recovered in the permeate via membrane filtration.⁵

322 The TN was expected to increase as the solids were solubilized. As seen in Figure 1d, the
323 average TN concentration in the permeate was 302.9 ± 38.6 mg/L as N between days 27 and 70.
324 After day 70, the concentration increased and peaked at 1165.4 mg/L as N on day 125. The
325 concentration did not increase immediately during the transient event, such as it did with DOC
326 and COD. Rather, it increased slowly over time as the TSS concentrations in R1 and R2
327 increased. The TN concentrations in the permeate were plotted versus the TSS concentration in
328 R2 and the data had a positive correlation with an R^2 value of 0.872 (see Figure S7), showing the
329 relationship between the increasing solids concentration in R2 and the release of soluble nitrogen
330 into the water phase, which was recovered in the permeate. On day 140, the solids concentration
331 in R2 was too high ($>20,000$ mg/L) to maintain the integrity of the membrane and the system
332 had to be shut down for complete removal of solids and reseeded for future runs of the system.

333 **3.2. Effects of the transient event on PMBR**

334 As the AnMBR experienced the transient event, the PMBR culture and water chemistry shifted
335 dramatically. It became evident that the increasing carbon had shifted the carbon-to-nitrogen
336 ratio in the RT contents that were fed to the PMBR. Figure 2 shows the carbon-to-nitrogen ratio
337 in the AnMBR permeate and the RT samples before, during, and after the transient event. Prior
338 to the event, the average C/N ratio was 0.62 and 0.33 in the AnMBR permeate and RT samples,
339 respectively, indicating that the AnMBR was removing carbon and releasing nitrogen as
340 expected. A low C/N ratio was desired because research has shown that low C/N ratios allow for
341 higher concentrations of nitrifying bacteria in a mixotrophic system.¹³ A low C/N ratio also
342 maintains a lower concentration of heterotrophic bacteria, which have higher growth rates
343 compared to nitrifiers and may cause reduced photosynthesis due to light shading.¹³ However,
344 due to the transient event, the C/N ratio in the permeate increased 22-fold from 0.34 to 1.77 from

345 day 34 to day 42, respectively. The C/N ratio increased steadily for the following 4 weeks of
346 sampling, finally peaking in the RT at 11.2, 34 times higher than the average C/N ratio prior to
347 the transient event. This was due to the dilution rate effect as contents from upstream tanks
348 influenced the concentrations of downstream tanks as a function of HRT. Slowly, the C/N ratio
349 started decreasing after day 70, returning to levels under 1.0 on day 131. The decrease was due to
350 a gradual decrease of carbon and an increase in the TN in the AnMBR permeate, as the system
351 recovered from the transient event and treated the contents in the reactor tanks. The C/N ratio
352 peak in the RT samples was offset by two weeks compared to the C/N ratio in the AnMBR
353 permeate samples (Figure 2). This was indicative of the HRT of the additional tank used to
354 integrate the AnMBR and the PMBR. The peak in the AnMBR permeate samples occurred on
355 day 55 and peaked at 12.1. Without an intermediary tank, such as the RT in our design, the
356 PMBR would have received a higher organic loading during the event and the effects of the
357 increased loading could have been greater than those seen in this study. This is an important
358 future consideration when designing robust systems for downstream treatment of wastewater
359 effluents.

360 As the C/N ratio increased, due to an increase in DOC concentration in the AnMBR
361 permeate, the reactor responded with a visible shift in the culture. The culture changed in color,
362 from the green color expected in a phototrophic bioreactor to a pale orange color that is more
363 indicative of a bacterial fermenter (see pictures in Figure S8). The change in the culture color
364 was also evident in the optical density (OD, 680 nm) data taken throughout the study period
365 (Figure 3). Prior to the peak in C/N ratio, the OD of the reactor increased as the culture density
366 increased. However, after the peak in C/N ratio, the OD began to drop, indicative of a drop in the
367 chlorophyll production in the reactor. This was true past the point at which the photoperiod was

368 changed on day 72, which occurred more than thirty days after the overload of solids started the
369 transient event. The OD reached the lowest level on day 94 and then began to increase as the
370 C/N ratio reached levels below 3. The change in the culture also affected the pH and DO
371 concentrations in the reactor, which increased to above pH 8 and decreased to below 1 mg/L
372 during this period (see Figure S9).

373 The water chemistry in the PMBR reactor and permeate samples also responded to the
374 changes. The AnMBR permeate that is used as the PMBR influent was high in $\text{NH}_4\text{-N}$ and
375 carbon concentrations. Initially, the goal of the study period was to assess the ability of PMBR to
376 perform nitrification of the AnMBR permeate. The $\text{NH}_4\text{-N}$ had three removal routes once in the
377 reactor: (1) biomass assimilation, (2) nitrification, and (3) volatilization at high pH. Prior to the
378 event, DOC, TN, $\text{NH}_3\text{-N}$, $\text{NO}_3\text{-N}$, and $\text{NO}_2\text{-N}$ were all nominal in the reactor and permeate
379 samples (Figure 4). The variations in the concentrations were due to the nominal start-up period
380 in which nitrification was occurring and biomass grew denser. Then, during the transient event,
381 the nitrate decreased to the background concentrations in the RT, indicating that nitrification was
382 no longer occurring. These data were used to calculate a nitrogen mass balance to determine the
383 fate of nitrogen in the liquid phase in the PMBR (Figure 5). The mass balance was normalized by
384 the influent TN (RT samples). The colloidal and dissolve fractions were calculated for
385 ammonium, nitrate, and nitrite. As seen in Figure 5, there was a large nitrite fraction in the first
386 two weeks of operation. As the operation continued into weeks 3 and 4, the nitrite fraction
387 decreased and the nitrate fraction increased. This was a direct measurement of nitrification taking
388 place. As the system stabilized, in weeks 5 and 6, the largest fraction of nitrogen was in the form
389 of dissolved nitrate, reaching levels up to 75% on day 42. Throughout this period, greater than

390 80% of the TN in the PMBR influent (RT) was in the form of $\text{NH}_4\text{-N}$. Therefore, in the first 6
391 weeks, ammonia removal was governed by biomass assimilation and nitrification, as expected.

392 As the C/N ratio increased, the mass balance showed that nitrification was inhibited, and
393 the system was not meeting the nitrification goal based on the shift in nitrogen fractions.

394 Beginning in week 7, the nitrogen mass balance began to show decreasing values in the
395 measured nitrogen fractions and an increase in the theoretical fraction. By week 9, more than
396 90% of the nitrogen mass balance was made up of the theoretical biomass uptake or nitrogen
397 volatilization fraction and it remained at an average of 85% for the next 9 weeks of operation.

398 The ammonia and the TN concentrations in the PMBR permeate during this period were about
399 25 mg/L as N and 50 mg/L, respectively. The nitrate concentration was low, the dissolved
400 oxygen concentration was below 1 mg/L, and the pH was above pH 8 during this period (see
401 Figure S9), indicating that the TN fraction was either lost to uptake by the culture or by ammonia
402 volatilization. Even though the reactor was no longer nitrifying the ammonia, the concentration
403 in the permeate did not pose a possible risk for $\text{NH}_4\text{-N}$ toxicity in downstream fertigation
404 applications. After day 126, when the C/N ratio decreased below 1, the measured nitrogen
405 fractions started increasing slowly; a sign that the reactor was recovering from the transient
406 event. A picture taken on day 130 (see Figure S8) showed that the culture had shifted back to
407 predominantly algae compared to the picture taken on day 64.

408 One parameter that was not negatively influenced throughout the transient event was the
409 PMBR permeate DOC concentration (Figure 6). As the C/N ratio increased, the DOC
410 concentrations in the RT reached 2474 mg/L, almost 30 times the concentration in the weeks
411 before the transient event. The shift in the culture discussed previously contributed to the near-
412 complete removal of the excess carbon load coming from the upstream AnMBR transient event.

413 Starting on day 42, the DOC removal by the PMBR was 92% on average until the end of the
414 study period. This showed that the PMBR acted as a valuable technology after the carbon
415 washout event of the upstream AnMBR system. The PMBR removed the incoming DOC and
416 continued producing permeate with the low DOC concentration. The average DOC concentration
417 in the PMBR permeate in the samples post-C/N ratio peak was 97.8 mg/L, which was within the
418 range of the DOC concentration for the AnMBR permeate during nominal operation (98.3 ± 9.6
419 mg/L). During the transient event, the PMBR reacted to the increased DOC concentration and
420 removed the excess carbon to levels that met the AnMBR requirement for carbon removal. The
421 primary goal of the PMBR (i.e., nitrification for fertigation) was not met, but the system met the
422 primary requirements for the AnMBR (i.e., carbon removal). As the C/N ratio recovered,
423 observations indicated that the culture shifted from pale orange to green with decreasing carbon
424 and increasing nitrogen in the AnMBR permeate (see Figure S8). The characterization of the
425 shift in the community structure will be discussed in the following section.

426 **3.3. Characterizing the shift in the PMBR microbial communities associated with the** 427 **transient event**

428 The microbial community structure of the PMBR was analyzed to confirm the observations that
429 shifts in the culture had occurred during and after the transient event. Samples for biological
430 analyses were taken from (1) the mother culture stock, (2) the reactor during the elevated C/N
431 ratio, and (3) the reactor after the transient event had passed. Samples were not taken prior to the
432 event due to the unforeseen nature of the transient event. The samples represented the microbial
433 communities in that location at the time when the sample was taken. They might not represent
434 the entire microbial community of the reactor. The samples taken after the transient event were
435 taken on the last possible day of operation to fully differentiate it from the sample taken during

436 the peak in the transient event. Figure S10 shows the initial analysis of the DNA sequencing
437 results pertaining to the diversity found in the samples. The Shannon diversity index is a
438 measurement of diversity within each sample. A higher Shannon diversity index indicated that
439 there was more diversity within the sample's community structure. The results showed that the
440 diversity within each sample was highest in the samples taken during the peak in the transient
441 event when compared to the samples taken from the mother culture stock. Alternatively, the
442 Shannon diversity index was similar in the samples after the transient event compared to the
443 diversity in the mother culture. These results indicated that the microbial community of the
444 culture shifted during the transient event and that there was a second shift after the transient
445 event had passed.

446 Beta diversity was used to compare the microbial communities across different samples.
447 More specifically, the principal coordinate analysis (PCoA) of the Bray-Curtis dissimilarities
448 was used to compare the similarities and differences between the samples. Samples that were
449 more similar to each other clustered in the same region. As seen in Figure S10, there were two
450 distinct groupings in the data: (1) the samples taken from the mother culture were clustered
451 separately from the samples taken from the reactor, both during and after the transient event, and
452 (2) the samples taken after the transient event (reactor post) were clustered closer together and
453 away from the samples taken during the transient event (reactor peak and biofilm). These results
454 indicated that there was marked changes in the culture (1) once it began treating AnMBR
455 permeate and (2) while it was experiencing the transient event.

456 Next, the data were analyzed to determine how the community structures changed due to
457 the transient event. A total of 73 phyla were identified in the samples from the bacteria,
458 eukaryote, archaea, and virus domains. Bacterial communities were the first to be analyzed

459 because two bacterial phyla were the two most abundant phyla in the samples: Proteobacteria
460 ($80\% \pm 14\%$) and Actinobacteria ($6.2\% \pm 1.0\%$). Figure 7 shows the relative abundance of
461 bacterial genera in the PMBR samples taken from the mother culture, the reactor, and its biofilm
462 during the transient event, and the reactor samples after the transient event had passed. The
463 larger bubbles are indicative of a higher relative abundance within each sample. Only genera
464 with a relative abundance above 1% are shown in the figure. The results confirm that there was a
465 difference in the bacterial community structures based on the transient event. The samples taken
466 during the transient event had a larger number of genera with relative abundances above 1%,
467 with 22 genera identified in the samples compared to 11 and 14 genera in the mother culture and
468 the post-transient events samples, respectively. The communities were then analyzed to
469 determine if the community structure had any connection to the reactor conditions. The most
470 abundant genus in the mother culture was *Sphingopyxis*, a genus containing species known for
471 environmental bioremediation.³³ During the transient event, the most abundant genera were
472 *Hydrogenophaga* and *Thauera*, which contain yellow-tinted, hydrogen-oxidizing species and
473 species that metabolize aromatic compounds in anoxic conditions, respectively.^{34,35}
474 *Hydrogenophaga* also have the ability to heterotrophic denitrify nitrate.³⁵ This correlated with
475 the conditions within the reactor, as the DO decreased with the increase in the microbial
476 overgrowth, the culture turned into a light-orange color, and the decreasing nitrate
477 concentrations. After the transient event, the most abundant genera were *Alicyclophilus*,
478 *Acidovorax*, and *Comamonas*, known for their use in bioremediation and denitrification in the
479 environment.³⁶⁻³⁸ These three genera were present in the samples taken during the transient
480 event, but were not present in the mother culture. Also, their relative abundance increased
481 compared to the samples taken during the transient event, indicating enrichment caused by that

482 the conditions post-transient event. Conversely, *Hydrogenophaga* and *Thauera* decreased in
483 abundance or were not present in abundances higher than 1% in the post-transient event samples.
484 *Mesorhizobium*, *Pseudomonas*, and *Streptomyces* were in similar abundances throughout all
485 samples taken for this study, indicating that they were not affected by the reactor conditions and
486 may contribute to the stability in the culture. Specifically, studies have shown that
487 *Mesorhizobium* have a high tolerance to stresses from temperature, salt, and pH levels.³⁹
488 *Pseudomonas* is a large genus that has a wide functional and environmental range in soils and
489 aquatic environments, and its versatility lends itself to applications in bioremediation and
490 biotechnology.⁴⁰ *Streptomyces* is a genus of ecologically diverse bacteria that have a large
491 affinity for mutualistic interactions, such as those found to provide resistance to biotic and
492 abiotic stresses in the rhizosphere of plants.⁴¹ Finally, five genera were present in every sample
493 that was taken from the PMBR (during and after the transient event) that were not present in the
494 mother culture. These genera (*Acidovorax*, *Alicyclophilus*, *Comamonas*, *Hydrogenophaga*, and
495 *Variovorax*) could be attributed to the influence of the AnMBR permeate on the PMBR culture,
496 as they were not present in the mother culture. Future research is needed to determine the
497 specific influence of the AnMBR cultures on downstream systems.

498 The sequencing results were analyzed for the presence of ammonia-oxidizing bacteria
499 (AOB) and nitrite-oxidizing bacteria (NOB) to determine the presence of nitrifiers in the samples
500 (see Figure S11). Of the seven NOB genera identified in the literature,⁴² only four were present
501 in the Kraken2 database used for this study and only three were identified in our samples
502 (*Nitrobacter*, *Candidatus Nitrotoga*, and *Nitrospira*). All three AOB genera were found in our
503 samples: *Nitrosococcus*, *Nitrosospira*, and *Nitrosomonas*. However, the mother culture samples
504 had a higher abundance of the NOB *Nitrobacter* and the reactor samples had a higher abundance

505 of the AOB *Nitrosomonas*. This could be due to the time between feedings of fresh media for the
506 mother culture compared to the constant introduction of AnMBR permeate in the PMBR system,
507 as HRT has a large influence on the growth rate of AOBs and NOBs.⁴³ The ratio of AOB to
508 NOB was calculated for each sample to determine whether the samples fell within 2.2–2.7,
509 which is the optimal range for nitrification (see Figure S11).⁴⁴ The results show that the ratio in
510 the reactor samples (during the transient event and after the transient event) were all greater than
511 2.7. The results for the mother culture were all below 2.2. This shows that the AOB content in
512 the reactor was outgrowing the NOBs, leading to accumulation of nitrite.⁴⁵ Nitrite spikes were
513 seen in the PMBR throughout this study (Figure 4d). In the mother culture, the results show that
514 the NOBs were more abundant than the AOBs, leading to accumulation of nitrate and a
515 possibility of a nitrite loop as denitrifiers reduce nitrate to nitrite for the NOB.^{46,47}

516 Phyla containing fungi and the cyanobacteria phyla made up a max of 0.8% and 1.14%,
517 respectively, of the phyla present in the samples. The genera-level analysis was done for fungi
518 and cyanobacteria (see Figure S12 and S13) and the most abundant fungi and cyanobacteria were
519 maintained throughout all the samples. Seven fungi genera were found in every sample
520 sequenced: *Purpureocillium*, *Therموthelomyces*, *Colletotrichum*, *Therموthielavioides*,
521 *Pyricularia*, *Fusarium*, and *Aspergillus*. The change in the C/N ratio did not seem to influence
522 the most abundant community members in the samples collected during and after the transient
523 event, but it did influence their relative abundance. A recent study showed that the treatment
524 efficiency of a fungal reactor increased with decreasing C/N ratio.⁴⁸ Future research is needed to
525 determine the effects of the fungi population in a mixed culture, such as the one used in this
526 study. Three cyanobacteria genera were found in all the samples taken (*Synechococcus*, *Nostoc*,
527 and *Calothrix*) and one genus was found only in the samples taken from the reactor

528 (*Gloeobacter*). Cyanobacteria have been identified as organisms that may be found on extra-
529 terrestrial systems because they have a wide variety of adaptations to extreme environments,
530 coming from their long evolutionary history.⁴⁹ Specifically, *Gloeobacter* have photosynthetic
531 systems closely related to primitive organisms, are slow growers, and tend to aggregate in
532 mats.⁵⁰ Their aggregation to the reactor surfaces may be a reason why they were identified in the
533 reactor samples and not in the mother culture.

534 **3.4. Implications of BLiSS operations on reliability and robustness for Lunar and Martian** 535 **habitats**

536 This research has shown that PMBR treatment may be a viable post-treatment of AnMBR
537 permeate because its robust community is able to respond to variable water quality in the
538 AnMBR permeate during transient events. The culture adapted to the increased carbon level
539 during the transient event and rebounded to its initial condition when the AnMBR returned to
540 nominal conditions. The use of an algal–bacterial consortium and the physical barrier, i.e., the
541 UF membrane, were key in allowing for the shift to occur. The bacteria responded to increased
542 carbon concentrations, removed the carbon to acceptable levels, and was out-competed by the
543 algae once the incoming carbon levels rebounded to nominal concentrations. Without the
544 physical barrier, the algae could have been washed out, making a shift in the community
545 impossible after the carbon rebounded to background concentrations. The parallel treatment of
546 wastewater with an AnMBR followed by a PMBR increased the resilience of the entire system,
547 as the PMBR responded to an anomaly in treatment in the AnMBR and continued the production
548 of a low-carbon permeate. While the PMBR had its own goal of nitrifying the AnMBR permeate,
549 the PMBR provided the additional benefit of producing a low-carbon effluent while the AnMBR
550 was recovering from the transient event.

551 Resilience in engineering design, not to be confused with the resilience of the microbial
552 community, is defined as the ability to respond to an adverse event, with a strong emphasis on
553 reliability and restoration.⁵¹ Reliability and restoration are both influenced by the system's
554 robustness (i.e., the ability for a system to keep a failure from affecting downstream processes),
555 its rapidity (i.e., the speed at which the system responds to the failure), and its redundance (i.e.,
556 the availability of critical components necessary to respond to the failure).⁵² In this case, the
557 resilience of the engineering design is closely tied to the resilience of the microbial community.
558 In microbial communities, resistance and resilience are guided by the communities' response to
559 external stimuli by the response of the individuals, the population's persistence, and community
560 stability.⁵³ Additionally, the characteristics of the disturbance on the community, such as its
561 intensity, the nature of the disturbance, the time interval between disturbances, and the order of the
562 disturbance, may influence the time it takes to recover from the disturbance.⁵⁴ Proper
563 engineering design and microbial community stability are needed to have a resilient BLiSS
564 architecture. Based on these definitions, the PMBR was able to provide added resilience to the
565 engineering design of treatment architecture because it was reliable during the event and allowed
566 for the AnMBR system to return to nominal conditions. While the system did lose its ability to
567 nitrify the AnMBR permeate, the downstream fertigation system should also include engineering
568 controls to increase robustness. While the design of the fertigation system is out of the scope of
569 this paper, there are many methods for mitigating variable nitrogen speciation including shifting
570 nitrite to nitrate via room air bubbling, inclusion of a biofilter in the nutrient solution
571 recirculation loop, and biochar absorption of ammonia prior to the fertigation system.⁵⁵⁻⁵⁷
572 Elevated carbon concentrations would be detrimental to these technologies and having the
573 removal of carbon prior to their implementation is key for hydroponics systems.

574 Resilience in BLiSS is going to be paramount for a sustained human presence on
575 extraplanetary bases. These systems must be able to respond to anomalies in treatment while still
576 providing the necessary service to the crew. Hence, an approach of designing systems in-series
577 and in-parallel should be explored. Systems designed in-series, such as the AnMBR and the
578 PMBR in this study, are designed to provide resilience within the treatment train. Systems that
579 are designed in-parallel, such as two treatment trains of AnMBRs followed by PMBRs, would be
580 designed to provide reliance to the BLiSS system. If one treatment train were to face an anomaly,
581 the other system could respond and provide the necessary service for the habitat. However, this
582 has major implications for mass and volume requirements, as increasing the mass and volume of
583 a technology makes it less favorable for integration into the final architecture designs due to cost
584 constraints. Future work is needed on how resilience informs trade studies and how designing in-
585 series and in-parallel affects the overall efficiency of the system.

586 **4. Conclusion**

587 AnMBRs have been proposed as solutions for decentralized wastewater treatment in resource-
588 limited, remote locations. However, AnMBRs are limited by their inability to remove nutrients.
589 When paired with algal–bacterial PMBRs, algal photosynthesis provides the necessary dissolved
590 oxygen for bacterial nitrification. In this research, the effects of increasing C/N ratio in the
591 AnMBR permeate on PMBR water quality and microbial communities were shown. The PMBR
592 culture shifted during the transient event, allowing for the continued removal of carbon to meet
593 the requirements of the AnMBR. The shift allowed for the AnMBR to recover from the increased
594 carbon load and the PMBR shifted back to a predominant algal culture after the C/N ratio
595 decreased to below 3. Shotgun metagenomics showed marked differences in the microbial
596 communities during and after the transient event, strengthening the importance of using

597 membrane technologies to maintain a robust culture of algae and bacteria for the treatment of
598 complex wastewater. This research gives insight into the additional robustness that PMBRs
599 provide to wastewater treatment with AnMBRs. Future research is needed to evaluate the cost
600 and benefits of designing a system with redundancy in terms of mass, volume, and economic
601 costs, especially as it pertains to failure modes and application of the technologies in remote,
602 extreme locations.

603 **Data Availability**

604 Raw data for the DNA sequencing can be found in the NASA Open Science Data Repository
605 with DOI: 10.26030/vmzd-0s72.

606 **Author Contributions**

607 **Daniella Saetta:** Conceptualization, Investigation, Data Curation, Formal Analysis,
608 Visualization, Writing - Original Draft. **Jason A. Fischer:** Conceptualization, Investigation,
609 Data Curation, Writing - Review & Editing. **Ashley Triana:** Investigation, Writing - Review &
610 Editing. **Talon Bullard:** Conceptualization, Investigation. **Alexandra Smith:** Conceptualization,
611 Writing - Review & Editing. **Cory J. Sporn:** Investigation. **Anirudha Dixit:** Data Curation,
612 Formal Analysis. **Christina L. Khodadad:** Formal Analysis, Resources, Writing - Review &
613 Editing. **Daniel H. Yeh:** Conceptualization, Resources, Writing - Review & Editing,
614 Supervision, Funding acquisition. **Luke B. Roberson:** Conceptualization, Resources,
615 Supervision, Writing - Review & Editing, Project administration, Funding acquisition.

616 **Conflict of Interest**

617 Luke Roberson has patent #20230271865 pending to UNITED STATES OF AMERICA AS
618 REPRESENTED BY THE ADMINISTRATOR OF NASA. Daniel Yeh has patent #11891321
619 issued to University of South Florida, UNITED STATES OF AMERICA AS REPRESENTED

620 BY THE ADMINISTRATOR OF NASA. If there are other authors, they declare that they have
621 no known competing financial interests or personal relationships that could have appeared to
622 influence the work reported in this paper.

623 **Acknowledgments**

624 This work was supported by the NASA Mars Campaign Office. The authors would like to thank
625 the support of those at the NASA Kennedy Space Center and University of South Florida who
626 made this work possible. The authors would like to thank the four anonymous reviewers who
627 provided thoughtful comments in the review process.

628 **References**

- 629 1 X. F. Almansa, R. Starostka, L. Raskin, G. Zeeman, F. De Los Reyes, J. Waechter, D. Yeh and T.
630 Radu, Anaerobic digestion as a core technology in addressing the global sanitation crisis: challenges
631 and opportunities, *Environ. Sci. Technol.*, 2023, **57**, 19078–19087.
- 632 2 G. Skouteris, D. Hermosilla, P. López, C. Negro and Á. Blanco, Anaerobic membrane bioreactors for
633 wastewater treatment: A review, *Chemical Engineering Journal*, 2012, **198–199**, 138–148.
- 634 3 Z. An, J. Zhu, M. Zhang, Y. Zhou, X. Su, H. Lin and F. Sun, Anaerobic membrane bioreactor for the
635 treatment of high-strength waste/wastewater: A critical review and update, *Chemical Engineering*
636 *Journal*, 2023, **470**, 144322.
- 637 4 A. L. Smith, L. B. Stadler, L. Cao, N. G. Love, L. Raskin and S. J. Skerlos, Navigating wastewater
638 energy recovery strategies: a life cycle comparison of anaerobic membrane bioreactor and
639 conventional treatment systems with anaerobic digestion, *Environ. Sci. Technol.*, 2014, **48**, 5972–
640 5981.
- 641 5 A. L. Smith, L. B. Stadler, N. G. Love, S. J. Skerlos and L. Raskin, Perspectives on anaerobic
642 membrane bioreactor treatment of domestic wastewater: A critical review, *Bioresource Technology*,
643 2012, **122**, 149–159.
- 644 6 X. Song, W. Luo, F. I. Hai, W. E. Price, W. Guo, H. H. Ngo and L. D. Nghiem, Resource recovery
645 from wastewater by anaerobic membrane bioreactors: Opportunities and challenges, *Bioresource*
646 *Technology*, 2018, **270**, 669–677.
- 647 7 J. D. Lea-Cox, G. W. Stutte, W. L. Berry and R. M. Wheeler, Charge balance--a theoretical basis for
648 modulating pH fluctuations in plant nutrient delivery systems, *Life Support Biosph Sci*, 1996, **3**, 53–59.
- 649 8 D. Savvas, E. Giannothanasis, T. Ntanas, I. Karavidas and G. Ntatsi, State of the art and new
650 technologies to recycle the fertigation effluents in closed soilless cropping systems aiming to maximise
651 water and nutrient use efficiency in greenhouse crops, *Agronomy*, 2023, **14**, 61.
- 652 9 J. González-Camejo, R. Barat, M. V. Ruano, A. Seco and J. Ferrer, Outdoor flat-panel membrane
653 photobioreactor to treat the effluent of an anaerobic membrane bioreactor. Influence of operating,
654 design, and environmental conditions, *Water Science and Technology*, 2018, **78**, 195–206.
- 655 10 A. Prieto, PhD Dissertation, University of South Florida, 2011.
- 656 11 D. Saetta, J. A. Fischer, T. Bullard, A. Smith, J. R. Finn, L. Koss, O. Monje, D. H. Yeh and L.
657 Roberson, in *International Conference on Environmental Systems*, 2022.
- 658 12 A. Sial, B. Zhang, A. Zhang, K. Liu, S. A. Imtiaz and N. Yashir, Microalgal–bacterial synergistic

- 659 interactions and their potential influence in wastewater treatment: a review, *Bioenerg. Res.*, 2021, **14**,
660 723–738.
- 661 13 A. Fallahi, F. Rezvani, H. Asgharnejad, E. Khorshidi Nazloo, N. Hajinajaf and B. Higgins, Interactions
662 of microalgae-bacteria consortia for nutrient removal from wastewater: A review, *Chemosphere*, 2021,
663 **272**, 129878.
- 664 14 J. González-Camejo, S. Aparicio, M. Pachés, L. Borrás and A. Seco, Comprehensive assessment of the
665 microalgae-nitrifying bacteria competition in microalgae-based wastewater treatment systems:
666 Relevant factors, evaluation methods and control strategies, *Algal Research*, 2022, **61**, 102563.
- 667 15 M. Zhang, K.-T. Leung, H. Lin and B. Liao, Effects of solids retention time on the biological
668 performance of a novel microalgal-bacterial membrane photobioreactor for industrial wastewater
669 treatment, *Journal of Environmental Chemical Engineering*, 2021, **9**, 105500.
- 670 16 T.-D.-H. Vo, M.-D.-T. Pham, B.-T. Dang, C.-S. Tran, T.-S. Le, V.-T. Nguyen, T.-B. Nguyen, C. Lin,
671 S. Varjani, T.-S. Dao, T.-V. Bui, K.-P.-H. Huynh and X.-T. Bui, Influence of nitrogen species and
672 biomass retention time on nutrient removal and biomass productivity in a microalgae-based bioreactor,
673 *Environmental Technology & Innovation*, 2022, **28**, 102880.
- 674 17 Y.-K. Lee, Microalgal mass culture systems and methods: Their limitation and potential, *Journal of*
675 *Applied Phycology*, 2001, **13**, 307–315.
- 676 18 J. J. Werner, D. Knights, M. L. Garcia, N. B. Scalfone, S. Smith, K. Yarasheski, T. A. Cummings, A.
677 R. Beers, R. Knight and L. T. Angenent, Bacterial community structures are unique and resilient in
678 full-scale bioenergy systems, *Proc. Natl. Acad. Sci. U.S.A.*, 2011, **108**, 4158–4163.
- 679 19 E. E. Matula and J. A. Nabity, Failure modes, causes, and effects of algal photobioreactors used to
680 control a spacecraft environment, *Life Sciences in Space Research*, 2019, **20**, 35–52.
- 681 20 J. A. Fischer, D. Saetta, J. Finn, T. Bullard, A. Smith, L. Koss, O. Monje, D. H. Yeh and L. Roberson,
682 in *International Conference on Environmental Systems*, 2022.
- 683 21 M. T. Pickett, L. B. Roberson, J. L. Calabria, T. J. Bullard, G. Turner and D. H. Yeh, Regenerative
684 water purification for space applications: Needs, challenges, and technologies towards ‘closing the
685 loop’, *Life Sciences in Space Research*, 2020, **24**, 64–82.
- 686 22 P. Clauwaert, M. Muys, A. Alloul, J. De Paepe, A. Luther, X. Sun, C. Ilgrande, M. E. R. Christiaens,
687 X. Hu, D. Zhang, R. E. F. Lindeboom, B. Sas, K. Rabaey, N. Boon, F. Ronsse, D. Geelen and S. E.
688 Vlaeminck, Nitrogen cycling in Bioregenerative Life Support Systems: Challenges for waste refinery
689 and food production processes, *Progress in Aerospace Sciences*, 2017, **91**, 87–98.
- 690 23 N. Sueoka, Mitotic replication of deoxyribonucleic acid in *Chlamydomonas reinhardi*, *Proc. Natl.*
691 *Acad. Sci. U.S.A.*, 1960, **46**, 83–91.
- 692 24 S.-W. Hwang and G. A. Hudock, Synchronously grown cultures of *Chlamydomonas reinhardi*, *J*
693 *Phycol.*, 1971, **7**, 300–303.
- 694 25 S. Surzycki, in *Methods in Enzymology*, Elsevier, 1971, vol. 23, pp. 67–73.
- 695 26 J. Lindholm, P. Gustafsson and G. Öquist, Photoinhibition of photosynthesis and its recovery in the
696 green alga *chlamydomonas reinhardii*, *Plant and Cell Physiology*,
697 DOI:10.1093/oxfordjournals.pcp.a077393.
- 698 27 T. Bullard, A. Smith, B. Hoque, R. Bair, M. Delgado-Navarro, P. Long, A. E. Uman, M. Pickett, D. H.
699 Yeh and L. Roberson, in *International Conference on Environmental Systems*, 2021.
- 700 28 A. L. Prieto, C. S. Criddle and D. H. Yeh, Complex organic particulate artificial sewage (Copas) as
701 surrogate wastewater in anaerobic assays, *Environ. Sci.: Water Res. Technol.*, 2019, **5**, 1661–1671.
- 702 29 J. Law, M. Van Baalen, M. Foy, S. S. Mason, C. Mendez, M. L. Wear, V. E. Meyers and D.
703 Alexander, Relationship between carbon dioxide levels and reported headaches on the international
704 space station, *Journal of Occupational & Environmental Medicine*, 2014, **56**, 477–483.
- 705 30 D. Saetta, J. A. Fischer, T. Bullard, A. Smith, C. J. Sporn, A. Dixit, C. Khodadad, D. H. Yeh and L.
706 Roberson, in *International Conference on Environmental Systems*, 2023.
- 707 31 D. Jun, Y. Kim, S. Hafeznezami, K. Yoo, E. M. V. Hoek and J. Kim, Biologically induced
708 mineralization in anaerobic membrane bioreactors: Assessment of membrane scaling mechanisms in a
709 long-term pilot study, *Journal of Membrane Science*, 2017, **543**, 342–350.

- 710 32 Z. Wu, W. Qiao, Y. Liu, J. Yao, C. Gu, X. Zheng and R. Dong, Contribution of chemical precipitation
711 to the membrane fouling in a high-solids type anaerobic membrane bioreactor treating OFMSW
712 leachate, *Journal of Membrane Science*, 2022, **647**, 120298.
- 713 33 M. Sharma, H. Khurana, D. N. Singh and R. K. Negi, The genus *Sphingopyxis*: Systematics, ecology,
714 and bioremediation potential - A review, *Journal of Environmental Management*, 2021, **280**, 111744.
- 715 34 B. Liu, Å. Frostegård and J. P. Shapleigh, Draft genome sequences of five strains in the genus *thauera*,
716 *Genome Announc*, 2013, **1**, e00052-12.
- 717 35 A. Willems, J. Busse, M. Goor, B. Pot, E. Falsen, E. Jantzen, B. Hoste, M. Gillis, K. Kersters, G.
718 Auling and J. De Ley, *Hydrogenophaga*, a new genus of hydrogen-oxidizing bacteria that includes
719 *hydrogenophaga flava* comb. Nov. (Formerly *Pseudomonas flava*), *hydrogenophaga palleronii*
720 (Formerly *Pseudomonas palleronii*), *hydrogenophaga pseudoflava* (Formerly *Pseudomonas*
721 *pseudoflava* and ‘*Pseudomonas carboxydoflava*’), and *hydrogenophaga taeniospiralis*(Formerly
722 *Pseudomonas taeniospiralis*), *International Journal of Systematic Bacteriology*, 1989, **39**, 319–333.
- 723 36 A. Willems and M. Gillis, in *Bergey’s Manual of Systematics of Archaea and Bacteria*, ed. W. B.
724 Whitman, Wiley, 1st edn., 2015, pp. 1–16.
- 725 37 Y. Wu, N. Zaiden and B. Cao, The core- and pan-genomic analyses of the genus *comamonas*: from
726 environmental adaptation to potential virulence, *Front. Microbiol.*, 2018, **9**, 3096.
- 727 38 C. J. Solís-González and H. Loza-Tavera, *alicycliphilus* : current knowledge and potential for
728 bioremediation of xenobiotics, *J Appl Microbiol*, 2019, **126**, 1643–1656.
- 729 39 M. Laranjo and S. Oliveira, Tolerance of *Mesorhizobium* type strains to different environmental
730 stresses, *Antonie van Leeuwenhoek*, 2011, **99**, 651–662.
- 731 40 M. W. Silby, C. Winstanley, S. A. C. Godfrey, S. B. Levy and R. W. Jackson, *Pseudomonas* genomes:
732 diverse and adaptable, *FEMS Microbiol Rev*, 2011, **35**, 652–680.
- 733 41 F. Pang, M. K. Solanki and Z. Wang, *Streptomyces* can be an excellent plant growth manager, *World J*
734 *Microbiol Biotechnol*, 2022, **38**, 193.
- 735 42 H. Daims, S. Lücker and M. Wagner, A new perspective on microbes formerly known as nitrite-
736 oxidizing bacteria, *Trends in Microbiology*, 2016, **24**, 699–712.
- 737 43 C. S. Gee, J. T. Pfeffer and M. T. Suidan, *Nitrosomonas and Nitrobacter* Interactions in Biological
738 Nitrification, *J. Environ. Eng.*, 1990, **116**, 4–17.
- 739 44 B. Li, S. Irvin and K. Baker, The variation of nitrifying bacterial population sizes in a sequencing
740 batch reactor (SBR) treating low, mid, high concentrated synthetic wastewater, *Journal of*
741 *Environmental Engineering and Science*, 2007, **6**, 651–663.
- 742 45 Q. Yao and D.-C. Peng, Nitrite oxidizing bacteria (NOB) dominating in nitrifying community in full-
743 scale biological nutrient removal wastewater treatment plants, *AMB Expr*, 2017, **7**, 25.
- 744 46 J. González-Camejo, P. Montero, S. Aparicio, M. V. Ruano, L. Borrás, A. Seco and R. Barat, Nitrite
745 inhibition of microalgae induced by the competition between microalgae and nitrifying bacteria, *Water*
746 *Research*, 2020, **172**, 115499.
- 747 47 M. K. H. Winkler, J. P. Bassin, R. Kleerebezem, D. Y. Sorokin and M. C. M. Van Loosdrecht,
748 Unravelling the reasons for disproportion in the ratio of AOB and NOB in aerobic granular sludge,
749 *Appl Microbiol Biotechnol*, 2012, **94**, 1657–1666.
- 750 48 M. Badia-Fabregat, D. Lucas, T. Tuomivirta, H. Fritze, T. Pennanen, S. Rodríguez-Mozaz, D. Barceló,
751 G. Caminal and T. Vicent, Study of the effect of the bacterial and fungal communities present in real
752 wastewater effluents on the performance of fungal treatments, *Science of The Total Environment*,
753 2017, **579**, 366–377.
- 754 49 P. Jung, F. Harion, S. Wu, D. J. Nürnberg, F. Bellamoli, A. Guillen, M. Leira and M. Lakatos, Dark
755 blue-green: Cave-inhabiting cyanobacteria as a model for astrobiology, *Front. Astron. Space Sci.*,
756 2023, **10**, 1107371.
- 757 50 J. A. Raven and P. Sánchez-Baracaldo, *Gloeobacter* and the implications of a freshwater origin of
758 Cyanobacteria, *Phycologia*, 2021, **60**, 402–418.
- 759 51 B. D. Youn, C. Hu and P. Wang, Resilience-driven system design of complex engineered systems,
760 *Journal of Mechanical Design*, 2011, **133**, 101011.

- 761 52 C. A. MacKenzie and C. Hu, Decision making under uncertainty for design of resilient engineered
762 systems, *Reliability Engineering & System Safety*, 2019, **192**, 106171.
- 763 53 A. Shade, H. Peter, S. D. Allison, D. L. Baho, M. Berga, H. Bürgmann, D. H. Huber, S. Langenheder,
764 J. T. Lennon, J. B. H. Martiny, K. L. Matulich, T. M. Schmidt and J. Handelsman, Fundamentals of
765 Microbial Community Resistance and Resilience, *Front. Microbio.*, DOI:10.3389/fmicb.2012.00417.
- 766 54 L. Philippot, B. S. Griffiths and S. Langenheder, Microbial Community Resilience across Ecosystems
767 and Multiple Disturbances, *Microbiol Mol Biol Rev*, 2021, **85**, e00026-20.
- 768 55 M. H. Su, E. Azwar, Y. Yang, C. Sonne, P. N. Y. Yek, R. K. Liew, C. K. Cheng, P. L. Show and S. S.
769 Lam, Simultaneous removal of toxic ammonia and lettuce cultivation in aquaponic system using
770 microwave pyrolysis biochar, *Journal of Hazardous Materials*, 2020, **396**, 122610.
- 771 56 D. Tanikawa, Y. Nakamura, H. Tokuzawa, Y. Hirakata, M. Hatamoto and T. Yamaguchi, Effluent
772 treatment in an aquaponics-based closed aquaculture system with single-stage nitrification–
773 denitrification using a down-flow hanging sponge reactor, *International Biodeterioration &
774 Biodegradation*, 2018, **132**, 268–273.
- 775 57 K. Thakur, T. Kuthiala, G. Singh, S. K. Arya, C. B. Iwai, B. Ravindran, K. S. Khoo, S. W. Chang and
776 M. K. Awasthi, An alternative approach towards nitrification and bioremediation of wastewater from
777 aquaponics using biofilm-based bioreactors: A review, *Chemosphere*, 2023, **316**, 137849.

778

779

780

781

782

783

784

785

786

787

788

789

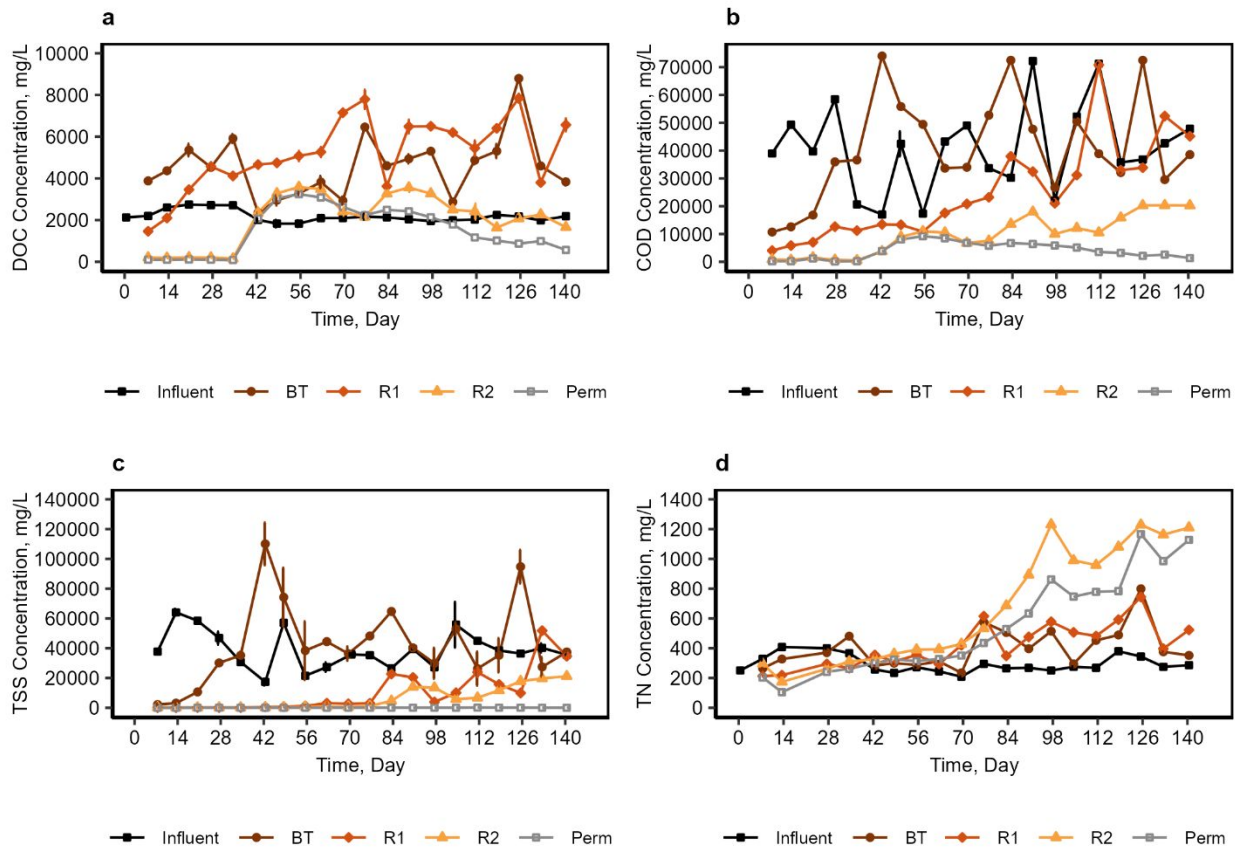
790

791

792

793

794 **Tables and Figures**



795

796 Figure 1 – (a) Dissolved organic carbon (DOC), (b) total chemical oxygen demand (COD), (c)
 797 total suspended solids (TSS) concentrations, and (d) TN concentrations in the AnMBR samples.

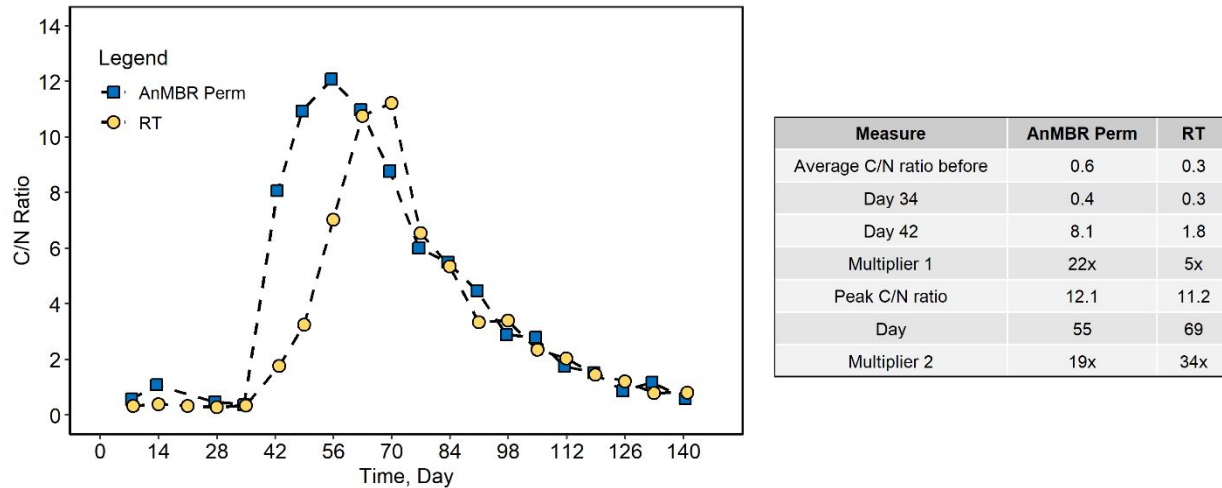
798 Error bars show the standard deviation in the sample triplicates.

799

800

801

802



803

804 Figure 2 – C/N ratio of the anaerobic membrane bioreactor (AnMBR) permeate and the reservoir
 805 tank (RT). Table shows a comparison of the C/N ratio values for the AnMBR perm and the RT
 806 samples. Multiplier 1 corresponds to the amount by which the value on Day 42 increased in
 807 comparison to the value on Day 34. Multiplier 2 corresponds to the amount by which the value
 808 on the peak increased in comparison to the average value before the transient event.

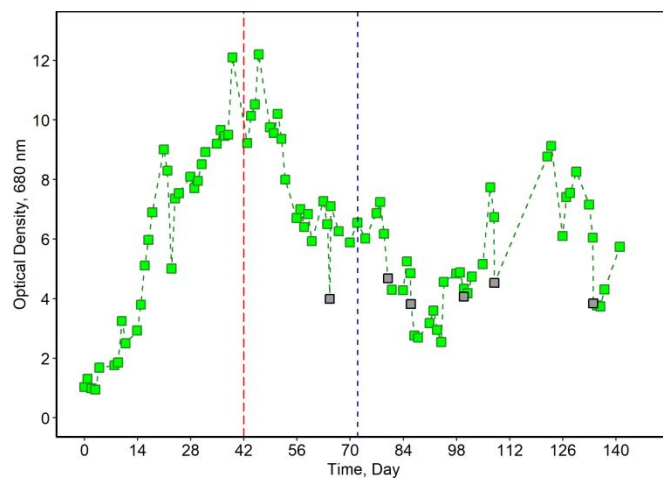
809

810

811

812

813

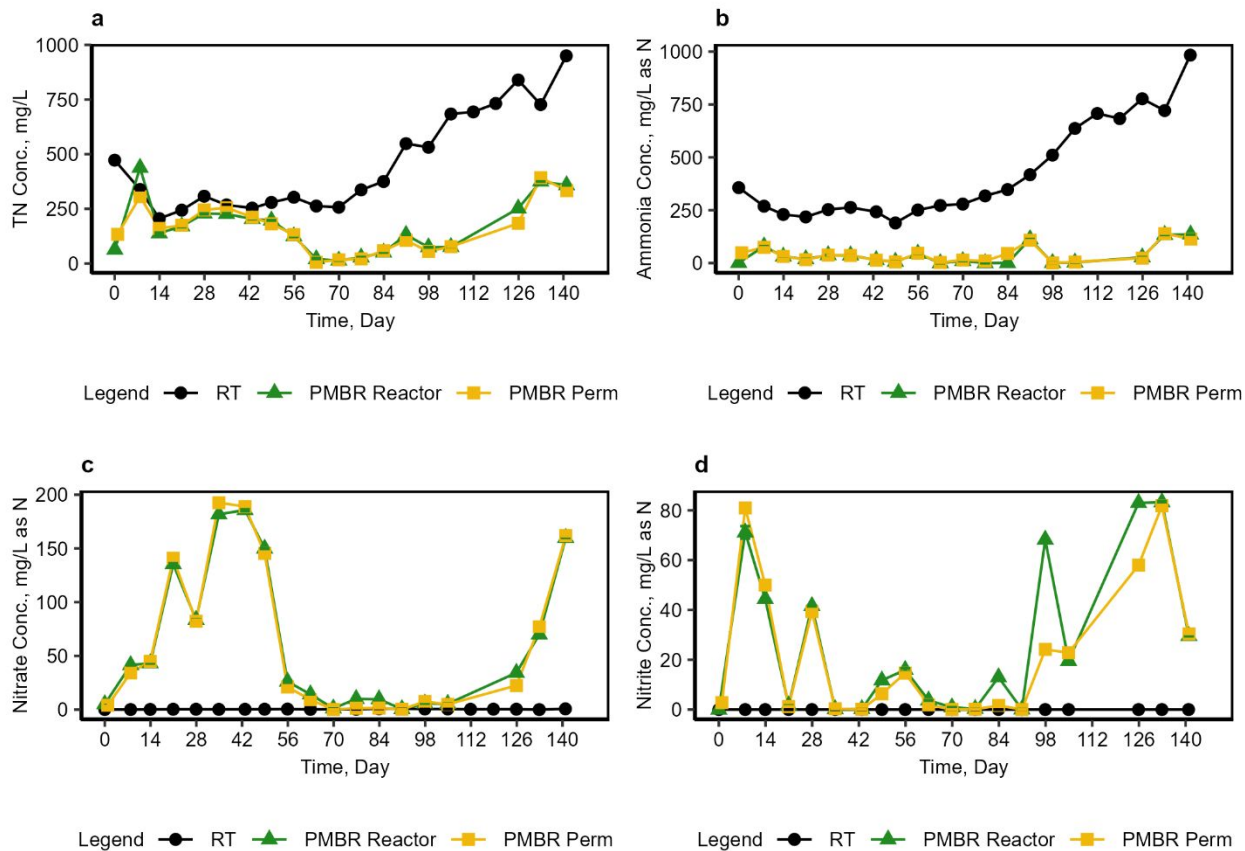


814

815 Figure 3 – Optical density (OD) at 680 nm of the phototrophic membrane bioreactor (PMBR)
816 reactor culture. The dark grey squares correspond to the OD measurements taken after harvesting
817 events. The red dashed line represents the peak in C/N ratio and the blue dashed line represents
818 the change in light photoperiods.

819

820



821

822 Figure 4 – (a) Total nitrogen (TN), (b) ammonia, (c) nitrate, and (d) nitrite in the RT, PMBR

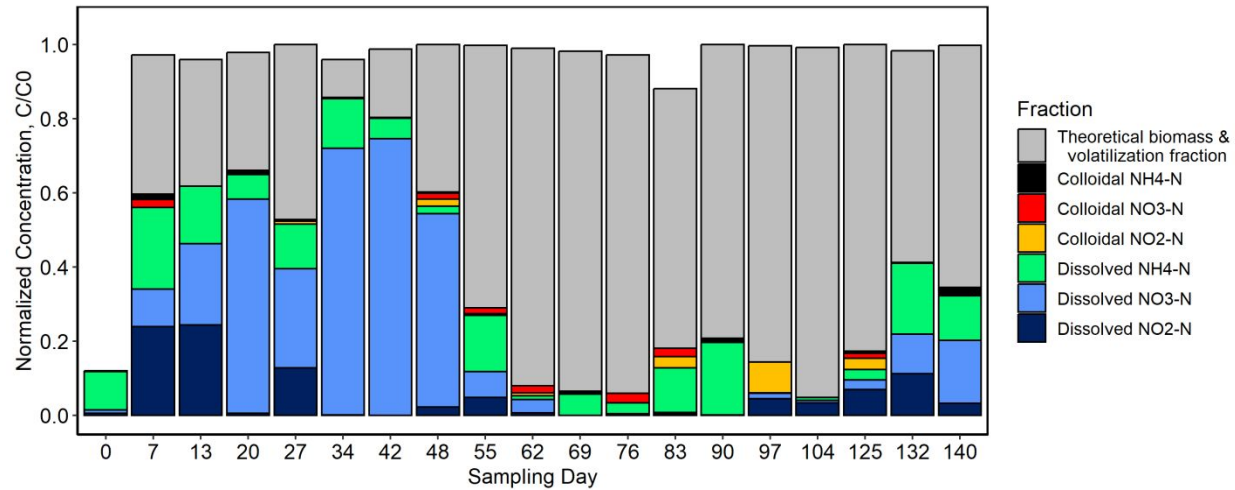
823 reactor, and PMBR perm samples. Error bars show the standard deviation of the sample

824 replicates.

825

826

827



828

829 Figure 5 – Nitrogen balance of the phototrophic membrane bioreactor (PMBR). The measured
830 colloidal and dissolved fractions of ammonia ($\text{NH}_4\text{-N}$), nitrate ($\text{NO}_3\text{-N}$), and nitrite ($\text{NO}_2\text{-N}$) are
831 shown. The theoretical biomass and volatilization fraction corresponds to the difference between
832 the sum of the measured fractions and the total nitrogen concentration in the PMBR influent.

833 Days 111 and 118 were not sampled. The concentrations used for this mass balance can be found
834 in the Table S3.

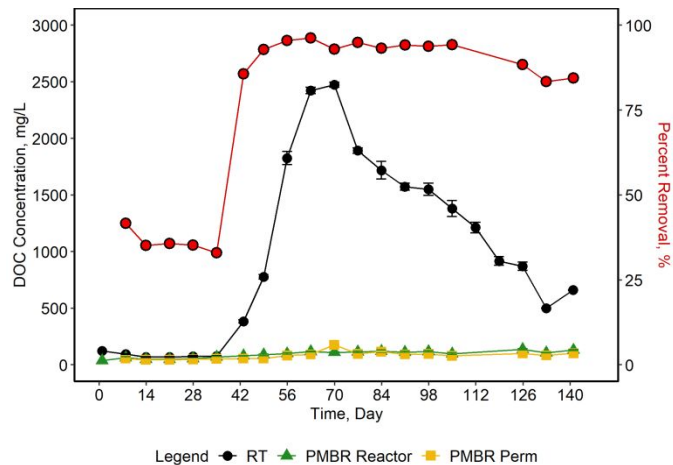
835

836

837

838

839



840

841 Figure 6 – Dissolved organic carbon (DOC) concentration in the reservoir tank (RT),
842 phototrophic membrane bioreactor (PMBR) reactor, and PMBR permeate samples. Percent
843 removal of DOC (red line and circles) is shown on the right axis. Error bars show the standard
844 deviation in the analytical duplicates.

845



846

847 Figure 7 – Bubble plot illustrating the bacterial genera diversity in the samples taken from the
 848 mother culture, reactor biofilm at the peak of the transient event, reactor contents at the peak of
 849 the transient event, and reactor contents after the transient event. Size of the bubble corresponds
 850 to the relative abundance percentage. Genera with a relative abundance below 1% are not shown
 851 in the figure.

Data Availability Statement

Raw data for the DNA sequencing can be found in the NASA Open Science Data Repository with DOI: [10.26030/vmzd-0s72](https://doi.org/10.26030/vmzd-0s72).